The Canadian Mineralogist
Vol. 34, pp. 1071-1088 (1996)

THE CRYSTAL STRUCTURE OF SCHOEPITE, $[(UO_2)_8O_2(OH)_{12}](H_2O)_{12}$

ROBERT J. FINCH[1], MARK A. COOPER AND FRANK C. HAWTHORNE

Department of Geological Sciences, University of Manitoba, Winnipeg, Manitoba R3T 2N2

RODNEY C. EWING

Department of Earth and Planetary Sciences, University of New Mexico, Albuquerque, New Mexico, 87131-1116, U.S.A.

Abstract

Schoepite, $[(UO_2)_8O_2(OH)_{12}](H_2O)_{12}$, is orthorhombic, *a* 14.337(3), *b* 16.813(5), *c* 14.731(4) Å, V 3551(2) Å^3, space group $P2_1ca$, $Z = 4$. The structure has been solved by direct methods and refined on F_o^2 to a weighted *R* index of 5.8% based on 4534 unique reflections measured with Mo$K\alpha$ X-radiation on a single-crystal diffractometer (equivalent to an *R* index of 2.7% for $F_o > 4\sigma F_o$). The refinement indicates that the formula contains eight more H_2O groups per unit cell than previously assumed. The structure consists of neutral $[(UO_2)_8O_2(OH)_{12}]$ sheets of edge- and corner-sharing $U\phi_7$ pentagonal dipyramids (ϕ: O, OH), hydrogen-bonded to each other through interstitial H_2O groups. These sheets are topologically identical to those found in fourmarierite. The $[(UO_2)_8O_2(OH)_{12}]$ sheets are interleaved with almost planar sheets of interlayer H_2O groups. There are twelve symmetrically distinct H_2O groups in the interlayer sheet; these are arranged in two pentagonal rings with two linking H_2O groups. H-atom positions were not resolved, but an H-bonding scheme is suggested on the basis of stereochemical and bond-valence arguments. The structure displays strong *Pbca* pseudosymmetry, especially among the U atoms. The lower symmetry is primarily due to H-bond interactions between interlayer H_2O groups and O(uranyl) atoms of the structural sheet.

Keywords: schoepite, crystal structure, uranium, hydrogen bonding, uranyl oxide hydrate.

Sommaire

La schoepite, $[(UO_2)_8O_2(OH)_{12}](H_2O)_{12}$, est orthorhombique, *a* 14.337(3), *b* 16.813(5), *c* 14.731(4) Å, V 3551(2) Å^3, groupe spatial $P2_1ca$, $Z = 4$. Nous en avons affiné la structure par méthodes directes en utilisant F_o^2 (4534 réflexions uniques mesurées avec rayonnement Mo$K\alpha$ par diffractométrie sur cristal unique), jusqu'à un résidu *R* de 5.8% (l'équivalent d'un indice *R* de 2.7% pour $F_o > 4\sigma F_o$). L'affinement montre que la formule contient huit groupes H_2O de plus par maille élémentaire que la formule acceptée ne l'indique. La structure contient des feuillets $[(UO_2)_8O_2(OH)_{12}]$ neutres de dipyramides pentagonales $U\phi_7$ à arêtes et à coins partagés (ϕ: O, OH), interliés entre eux par liaisons hydrogène assurées par les groupes H_2O interstitiels. Ces feuillets sont topologiquement identiques à ceux de la fourmarierite. Les feuillets $[(UO_2)_8O_2(OH)_{12}]$ sont intercalés avec des feuillets presque en plan de groupes H_2O. Il y a en tout douze groupes H_2O distincts dans ce feuillet interlité, agencés en deux anneaux pentagonaux liés par deux groupes H_2O. Nous n'avons pas affiné la position des atomes H, mais nous proposons quand même un schéma de liaisons hydrogène fondé sur arguments stéréochimiques et sur les valences de liaison. La structure montre une forte pseudo-symétrie *Pbca*, surtout parmi les atomes U. La symétrie inférieure est surtout due aux interactions des liaisons H entre les groupes H_2O des feuillets interlités et les atomes d'oxygène des groupes uranyle du feuillet structural.

(Traduit par la Rédaction)

Mots-clés: schoepite, structure cristalline, uranium, liaison hydrogène, oxyde d'uranyle hydraté.

Introduction

Schoepite was originally described by Walker (1923); its formula has been reported as $3UO_3{\cdot}7H_2O$ (Schoep 1932), $4UO_3{\cdot}9H_2O$ (Billiet & de Jong 1935, Schoep & Stradiot 1947) and $UO_3{\cdot}2H_2O$ (Christ & Clark 1960). The related mineral paraschoepite, $5UO_3{\cdot}9\frac{1}{2}H_2O$, was described by Schoep & Stradiot (1947). The relationship between paraschoepite and schoepite is uncertain (Christ & Clark 1960, Christ 1965). A third related mineral, metaschoepite, may be a lower hydrate than schoepite (Christ & Clark 1960). X-ray diffraction studies of synthetic UO_3 hydrates indicate only one phase related to schoepite; however,

[1] *E-mail address*: cfinch@cmt.anl.gov.

infrared spectroscopy and thermogravimetric analysis commonly suggest a second synthetic modification (Hoekstra & Siegel 1973). The chemical composition and structure of schoepite have been the subjects of much discussion (Baran 1992, Finch *et al.* 1992, Čejka & Urbanec 1990). Schoepite occurs at many oxidized uranium deposits, and it may play a key role in the paragenesis of the complex assemblage of uranyl minerals that form where uraninite has been exposed to oxidizing meteoric water (Finch *et al.* 1992, Deliens 1977a).

Recently, there has been renewed interest in the paragenesis and structure of uranyl oxide hydrates, particularly schoepite, ianthinite and becquerelite, as they not only occur as products of the secondary alteration of uraninite under oxidizing conditions (Finch & Ewing 1992, Frondel 1958), but are also prominent phases in laboratory experiments on alteration of the UO_2 of nuclear fuel (Johnson & Werme 1994, Forsyth & Werme 1992, Wronkiewicz *et al.* 1992, Stroes-Gascoyne *et al.* 1985, Wang & Katayama 1982, Wadsten 1977). Details of the occurrence of uranyl oxide hydrate minerals are an important test of the extrapolation of results of short-term experiments to periods relevant to nuclear-waste disposal (Ewing 1993). Moreover, they provide important constraints on models used to predict the long-term behavior of spent nuclear fuel (Bruno *et al.* 1995).

Experimental

We examined schoepite crystals from two museum samples, and data sets were collected on seven of these (Table 1). Five of these crystals were extracted from sample MRB B3616, in which a matrix of fine-grained (~1 μm) rutherfordine surrounds large (1–2 mm) blocky crystals of yellow schoepite and amber-colored becquerelite. A cleavage fragment was taken from one crystal of schoepite and checked optically before mounting on a glass fiber. After three days on the diffractometer, this crystal (*sc–a*) decomposed at its core to a polycrystalline powder, leaving only a donut-shaped fragment. Two more cleavage fragments were removed from the sample and examined by precession photography. One of these (*sc–b*) decomposed on the precession camera in a fashion similar to crystal *sc–a*. The second crystal (*sc–c*) changed from translucent yellow to opaque yellow during a ten-hour exposure, but remained intact. A precession photograph taken after this change showed significantly broadened diffraction-spots, changes in the diffracted intensities, and a 2% decrease in the *a* cell edge from 14.29 Å to ~14.0 Å. This is consistent with the alteration of schoepite to metaschoepite (Christ & Clark 1960).

Subsequent crystals taken from sample MRB B3616 were coated with hair spray after extraction in order to prevent alteration. This was partly successful, and the coated crystals remained translucent; however, data collected from four coated crystals were inadequate to solve the structure satisfactorily. The most reasonable solution and refinement were obtained using data from crystal *sc–d(2)*, but bond lengths and displacement factors were not reasonable. At this point, a second schoepite-bearing sample (CSM 91.62) was examined. This sample consisted of a coarsely crystalline matrix of intergrown schoepite, becquerelite, vandendriesscheite and ianthinite, in contact with altered uraninite and veined by soddyite and uranophane. Cleavage fragments were taken from inclusion-free crystals of schoepite that had grown within a cavity. Two of these were mounted on glass fibers and examined both optically and by precession photography. These two crystals were not coated, and they did not alter during the data collections; however, both *schoa* and *schob* eventually became polycrystalline approximately one year after extraction from sample CSM 91.62.

TABLE 1. UNIT-CELL PARAMETERS FOR SCHOEPITE CRYSTALS EXAMINED DURING THIS STUDY

		a	*b*	*c*	Sp. Gr.	Vol. (Å^3)	remarks‡
				MRB B3616			
	sc-a	14.301(3)	16.788(4)	14.712(4)	*Pb-a*	3532(3)	decomposed
†	sc-d	14.308(3)	16.793(2)	14.706(3)	*Pb-a*	3533(2)	(C) *U* positions only
*	sc-d(2)	14.296(3)	16.775(4)	14.713(4)	$P2_1ca$	3528(3)	(C) R_1 = 7%, poor U_{ij}
	sc-e	14.17(1)	16.74(1)	14.68(2)	*Pb-a*	3482(9)	(C) *U* positions only
	sc-f	14.074(7)	16.717(7)	14.70(1)	*Pbna*	3458(6)	(C) *U* positions only
				CSM 91.62			
	schoa	14.308(2)	16.808(3)	14.705(4)	*Pbca*	3536(2)	R_1 = 8%, poor U_{ij}
	schob	14.337(3)	16.813(5)	14.731(4)	$P2_1ca$	3551(2)	R_1 = 2.7% final solution

‡ Crystals marked with (C) were coated with hair spray after mounting.
† crystals *sc-b* and *sc-c* decomposed during precession examination
* *sc-d* and *sc-d(2)* are the same crystal, but data were recollected on *sc-d(2)* after 6 months

Data for crystal *schoa* proved inadequate for structure solution, with problems similar to those observed for crystal *sc–d(2)*. Data for the second cleavage fragment (*schob*) were then collected, and a more precise absorption-correction was obtained (see below). Crystal *schob* also had the largest unit-cell volume among the crystals examined (Table 1). We suspect that this reflects the lack of significant intergrown metaschoepite, which has a smaller unit-cell volume than schoepite (Christ & Clark 1960). The presence of metaschoepite can be inferred from the smaller *a* cell-edges found for the other six crystals (Table 1).

Precession photographs of crystal *schob* confirmed the orthorhombic symmetry and the space group *Pbca*, in agreement with Christ & Clark (1960). A thin plate, approximately triangular, 0.2 mm on each edge and 0.02 mm thick, was mounted on a Siemens *P*4 Nicolet *R*3*m* automated four-circle diffractometer equipped with a graphite monochromator and Mo$K\alpha$ X-radiation. Forty diffraction-maxima, 25 of which were between 35 and 60° 2θ, were centered, and the unit-cell dimensions were refined by least squares (Table 2). Following the collection of the intensity data, the crystal was re-centered, and the unit-cell parameters redetermined. Differences from previously determined values were within the reported standard deviations, indicating that the crystal had not undergone significant alteration during data collection.

Data were collected using the θ–2θ scan-mode and a variable scan-rate proportional to the peak intensity (minimum and maximum scan-speeds were 1.7 and 29.3° 2θ/min, respectively). A total of 11,147 reflections was measured over the range $4° \le 2\theta \le 60°$, with index ranges $0 \le h \le 20$, $0 \le k \le 23$, $-20 \le l \le 20$. Two standard reflections were measured after every fifty reflections. An empirical absorption-correction was applied, based on 71 psi-scans of each of fifteen diffraction-maxima at least every 5° 2θ from 7 to 60°, and chosen such that the diffraction vectors spanned one quadrant of the Ewald sphere. The crystal was modeled as a {001} plate, and reflections with a plate-glancing angle less than 7° were discarded. The absorption correction reduced *R*(azimuthal) from 22.8% to 2.0%. The remaining 8278 reflections were corrected for drift, Lorentz, polarization and background effects.

TABLE 2. MISCELLANEOUS INFORMATION FOR SCHOEPITE (CSM 91.62)

a (Å)	14.337(3)	crystal size (mm)	0.19 x 0.21 x 0.02
b	16.813(5)	radiation	Mo$K\alpha$/Gr
c	14.731(4)	Total no. of I_o	11,147
V (Å³)	3551(2)	No. of F_o^2	8278
Sp. Gr.	$P2_1ca$	Unique reflections	4535
Z	4	*R*(azimuthal) %	22.8 → 2.0
ρ_{calc}	4.87	*R*(merge) %	2.6
ρ_{meas}*	4.8	wR_2 (F_o^2) %	5.8
μ (mm^{-1})	36.47	R_1 ($\lvert F_o \rvert > 4\sigma_F$) %	2.7
		R_1 (all data) %	5.8
		No. parameters	235

Cell contents $4\{[(UO_2)_8O_2(OH)_{12}](H_2O)_{12}\}$

$R_1 = \Sigma(\lvert F_o \rvert - \lvert F_c \rvert)/\Sigma \lvert F_o \rvert$

$wR_2 = [\Sigma w(F_o^2 - F_c^2)^2 / \Sigma w(F_o^2)^2]^{½}$ $w = 1/\sigma^2(F_o^2) + [0.0249 \bullet (P^2)]^{-1}$

$P = [\{\max(0, F_o^2)\} + 2F_c^2]/3$

* Billiet & de Jong (1935)

Structure Solution and Refinement

The *U* sites were located in the space group *Pbca* by direct methods using the program SHELXTL (4.1); most of the O atoms in the structural unit were located from difference-Fourier maps. The structure was refined to an *R* index of 6.7% using |*F*|; however, we could not locate all the O atoms in space group *Pbca*, and the O(uranyl) atoms displayed (apparent) positional disorder about the U atoms. Structure refinements were then tried in three subgroups, $Pbc2_1$, $Pb2_1a$ and $P2_1ca$, using the *U* positions as starting points. Only in space group $P2_1ca$ were we able to locate all remaining O atoms from difference-Fourier maps. The disorder of the O(uranyl) atoms, apparent in space group *Pbca*, was resolved as discrete positions in $P2_1ca$. As only three (weak) reflections violate the *b* glide in space group *Pbca* (031, 051, 053; all "observed" at ~3σ), the choice of the non-centrosymmetric space-group, $P2_1ca$, is based on achieving a crystal-chemically realistic solution of the structure, rather than on systematic-absence violations.

The structure refined to an *R* index of 3.0% in $P2_1ca$; however, *U*(6), *U*(8) and several O atoms [O(16), *OH*(2), *OH*(12)] had unreasonable displacement factors ($U_{eq} \approx 0$). In particular, isotropic displacement-factors were strongly correlated for the sheet-atom pairs pseudosymmetrically related by a 2-fold rotation axis along [010] [*i.e.*, *U*(1)/*U*(5), *U*(2)/*U*(6), *U*(3)/*U*(7), *U*(4)/*U*(8), *O*(17)/O(18), *OH*(1)/OH(7), *OH*(2)/*OH*(8), *OH*(3)/*OH*(9), *OH*(4)/*OH*(10), *OH*(5)/*OH*(11), *OH*(6)/*OH*(12)]. This is probably the result of strong variable correlation due to the prominent pseudosymmetry combined with residual absorption problems.

The structure was then refined on F^2 using the program SHELXL–93. Isotropic-displacement factors of O atoms in the plane of the structural sheets (sheet O atoms), pseudosymmetrically related by $^{[010]}2_1$ in space group *Pbca*, were constrained to be equal (Table 3). Displacement factors for all other atoms were refined independently. This lowered the R_1 index slightly to 2.7%. An extinction coefficient was refined but found to be negligible. The final wR^2 index of 5.8% is based on all intensity data except the 0 9 0 reflection, which was omitted because of severe overlap (4534 data, 235 parameters). The final minimum and maximum

TABLE 3. FINAL PARAMETERS FOR SCHOEPITE

Site	*x*	*y*	*z*	$^*U_{eq}$
U(1)	0.2591(1)	0.5132(1)	0.7583(2)	111(4)
U(2)	0.0276(1)	0.3775(1)	0.7628(2)	136(4)
U(3)	0.2792(1)	0.7451(1)	0.7474(2)	123(4)
U(4)	-0.0008(1)	0.6127(1)	0.7497(2)	122(4)
U(5)	0.2797(1)	0.0134(1)	0.7406(2)	100(4)
U(6)	0.0117(1)	0.8772(1)	0.7631(1)	71(3)
U(7)	0.2607(1)	0.2450(1)	0.7520(2)	84(3)
U(8)	0.0398(1)	0.1132(1)	0.7500(2)	84(3)
O(1)	0.2786(13)	0.5016(10)	0.6402(13)	150(41)
O(2)	0.2473(12)	0.5218(12)	0.8791(16)	77(40)
O(3)	0.0229(12)	0.3409(10)	0.6490(12)	160(43)
O(4)	0.0302(13)	0.4156(9)	0.8724(12)	109(39)
O(5)	0.2344(16)	0.7381(11)	0.6367(15)	215(52)
O(6)	0.3262(13)	0.7618(10)	0.8593(14)	113(39)
O(7)	0.0162(18)	0.6487(15)	0.6383(20)	429(74)
O(8)	-0.0041(15)	0.5815(11)	0.8689(13)	99(45)
O(9)	0.3063(13)	0.0221(14)	0.6248(19)	198(52)
O(10)	0.2575(14)	-0.0092(11)	0.8559(15)	236(53)
O(11)	0.0124(15)	0.9067(10)	0.8803(13)	142(40)
O(12)	0.0057(11)	0.8446(10)	0.6484(11)	151(42)
O(13)	0.2249(16)	0.2533(12)	0.6364(18)	256(58)
O(14)	0.2980(16)	0.2352(11)	0.8685(14)	182(46)
O(15)	0.0431(17)	0.0800(13)	0.8616(16)	203(56)
O(16)	0.0345(11)	0.1425(9)	0.6332(12)	63(32)
O(17)	-0.1530(9)	0.6265(9)	0.7408(8)	103(13)
O(18)	0.1985(9)	0.1205(9)	0.7619(8)	103(13)
OH(1)	0.3412(10)	0.8803(10)	0.7036(10)	94(14)
OH(2)	0.4180(16)	0.4814(12)	0.7885(14)	111(13)
OH(3)	0.1612(12)	0.6457(101	0.7802(13)	123(13)
OH(4)	0.1578(14)	0.8270(11)	0.7948(15)	141(15)
OH(5)	-0.0372(10)	0.7429(9)	0.7985(13)	84(14)
OH(6)	0.1026(11)	0.5020(9)	0.7041(10)	87(13)
OH(7)	0.2083(10)	0.3751(10)	0.7845(10)	94(14)
OH(8)	0.1222(16)	-0.0209(12)	0.7053(15)	111(13)
OH(9)	0.3835(14)	0.1501(11)	0.7099(13)	123(14)
OH(10)	0.3881(14)	0.3213(11)	0.6980(15)	141(15)
OH(11)	0.0907(10)	0.2490(9)	0.8053(13)	84(14)
OH(12)	0.4422(11)	-0.0010(9)	0.7811(10)	87(13)
W(1)	0.3221(11)	-0.1226(12)	0.5227(15)	291(41)
W(2)	0.4091(10)	0.5197(8)	0.4790(11)	189(30)
W(3)	0.1703(11)	0.3499(10)	0.4761(13)	169(34)
W(4)	0.1874(15)	0.1324(11)	0.4837(15)	276(45)
W(5)	0.4822(13)	0.7469(11)	0.5139(16)	420(51)
W(6)	0.1038(14)	0.5038(10)	0.5341(14)	209(47)
W(7)	0.2434(12)	0.6184(12)	0.4811(15)	330(44)
W(8)	0.1451(13)	-0.0423(10)	0.5225(17)	501(60)
W(9)	0.3871(14)	0.1600(13)	0.5295(19)	456(68)
W(10)	0.3595(16)	0.3528(11)	0.5145(17)	329(52)
W(11)	0.0895(14)	0.7612(12)	0.4862(17)	493(58)
W(12)	0.4307(14)	0.0066(10)	0.4664(13)	194(46)

* $U_{eq} = U_{eq} \times 10^4$ (Å^2)

TABLE 4. BOND DISTANCES (Å) FOR SCHOEPITE

U(1)-O(1)	1.77(2)	*U*(5)-O(9)	1.76(3)
U(1)-O(2)	1.79(2)	*U*(5)-O(10)	1.77(2)
U(1)-OH(7)	2.46(2)	*U*(5)-OH(1)e	2.47(2)
U(1)-OH(2)	2.38(2)	*U*(5)-OH(8)	2.39(2)
U(1)-OH(3)	2.65(2)	*U*(5)-OH(9)	2.78(2)
U(1)-OH(6)	2.39(2)	*U*(5)-OH(12)	2.42(2)
U(1)-O(17)b	2.28(2)	*U*(5)-O(18)	2.17(2)
<*U*(1)-O>	2.25	<*U*(5)-O>	2.25
<*U*(1)-O(sheet)>	2.43	<*U*(5)-O(sheet)>	2.45
U(2)-O(3)	1.79(2)	*U*(6)-O(11)	1.80(2)
U(2)-O(4)	1.74(2)	*U*(6)-O(12)	1.78(2)
U(2)-OH(7)	2.61(1)	*U*(6)-OH(1)a	2.49(2)
U(2)-OH(2)a	2.47(2)	*U*(6)-OH(8)c	2.48(2)
U(2)-OH(10)a	2.29(2)	*U*(6)-OH(4)	2.31(2)
U(2)-OH(11)	2.42(2)	*U*(6)-OH(5)	2.42(2)
U(2)-OH(6)	2.51(2)	*U*(6)-OH(12)d	2.37(1)
<*U*(2)-O>	2.26	<*U*(6)-O>	2.24
<*U*(2)-O(sheet)>	2.46	<*U*(6)-O(sheet)>	2.42
U(3)-O(5)	1.76(2)	*U*(7)-O(13)	1.78(3)
U(3)-O(6)	1.80(2)	*U*(7)-O(14)	1.80(2)
U(3)-OH(1)	2.52(2)	*U*(7)-OH(7)	2.36(2)
U(3)-OH(3)	2.43(2)	*U*(7)-OH(9)	2.45(2)
U(3)-OH(4)	2.33(2)	*U*(7)-OH(10)	2.37(2)
U(3)-OH(5)b	2.72(2)	*U*(7)-OH(11)	2.56(2)
U(3)-O(17)b	2.23(1)	*U*(7)-O(18)	2.28(2)
<*U*(3)-O>	2.26	<*U*(7)-O>	2.23
<*U*(3)-O(sheet)>	2.45	<*U*(7)-O(sheet)>	2.40
U(4)-O(7)	1.77(2)	*U*(8)-O(15)	1.74(2)
U(4)-O(8)	1.83(2)	*U*(8)-O(16)	1.79(2)
U(4)-OH(2)a	2.56(2)	*U*(8)-OH(8)	2.63(2)
U(4)-OH(3)	2.43(2)	*U*(8)-OH(9)a	2.40(2)
U(4)-OH(5)	2.36(2)	*U*(8)-OH(11)	2.53(2)
U(4)-OH(6)	2.47(2)	*U*(8)-OH(12)a	2.42(2)
U(4)-O(17)	2.20(1)	*U*(8)-O(18)	2.29(1)
<*U*(4)-O>	2.23	<*U*(8)-O>	2.26
<*U*(4)-O(sheet)>	2.40	<*U*(8)-O(sheet)>	2.46
<<*U*-O>>	2.25(3	<<*U*-O(sheet)>>	2.43(1
<<*U*-O(uranyl)>	1.78(4)		

O(sheet): sheet oxygen, O(uranyl): uranyl oxygen. Equivalent positions: a: *x*−½, *y*, 1½−*z*; b: *x*+½, *y*, 1½−*z*; c: *x*, *y*+1, *z*; d: *x*−½, *y*+1, 1½−*z*; e: *x*, *y*−1, *z*

electron-densities in the difference-Fourier map are −1.51 and 1.76 *e*/Å^3, respectively. Most residual electron-density is associated with the *U* sites. The final atomic coordinates and displacement factors are given in Table 3, selected interatomic distances are listed in Table 4, a bond-valence table is given in Table 5, and proposed H-bonding interactions are summarized in Tables 6 and 7. Observed and calculated structure-factors and anisotropic displacement factors for the U atoms can be obtained from The Depository of Unpublished Data, CISTI, National Research Council, Ottawa, Ontario K1A 0S2.

Because refinements on F_o^2 are less common than those using $|F_o|$ in the mineralogical literature, some comment on this method is warranted. Refinement on F_o^2 avoids several sources of bias (Wilson 1976, Hirshfeld & Rabinovich 1973, Arnberg *et al.* 1976) and increases the data-to-parameter ratio by including all data. Estimated standard deviations are reduced because more information is used, and the likelihood of getting trapped in a local minimum during refinement

TABLE 5. BOND-VALENCE ARRANGEMENT* IN SCHOEPITE

	$U(1)$	$U(2)$	$U(3)$	$U(4)$	$U(5)$	$U(6)$	$U(7)$	$U(8)$	Σ	†Σ+H
O(1)	1.92								1.92	
O(2)	1.83								1.83	
O(3)		1.83							1.83	2.03
O(4)		2.06							2.06	
O(5)			1.96						1.96	2.09
O(6)			1.78						1.78	1.90
O(7)				1.92					1.92	2.03
O(8)				1.66					1.66	1.85
O(9)					1.96				1.96	
O(10)					1.92				1.92	
O(11)						1.78			1.78	1.86
O(12)						1.87			1.87	2.01
O(13)							1.87		1.87	2.00
O(14)							1.74		1.74	1.85
O(15)								2.06	2.06	2.22
O(16)								1.83	1.83	2.02
O(17)	0.65		0.71	0.75					2.11	
O(18)					0.80		0.65	0.63	2.08	
OH(1)			0.43		0.46	0.44			1.31	2.10
OH(2)	0.54	0.46		0.39					1.39	2.22
OH(3)	0.34		0.49	0.49					1.32	2.17
OH(4)			0.59			0.61			1.20	2.05
OH(5)			0.30	0.56		0.50			1.36	2.18
OH(6)	0.53	0.43		0.46					1.42	2.06
OH(7)	0.47	0.36					0.56		1.39	2.26
OH(8)					0.53	0.44		0.35	1.32	2.13
OH(9)					0.27		0.47	0.52	1.26	2.04
OH(10)		0.63					0.55		1.18	1.99
OH(11)		0.50					0.39	0.41	1.30	2.08
OH(12)					0.50	0.55		0.50	1.55	2.35
Σ	6.28	6.27	6.26	6.23	6.44	6.19	6.23	6.30		

* calculated with the parameters of Brown & Wu (1976)

† Bond-valence sums to O atoms with estimated H-bond contributions added, shown only for those O atoms involved in H-bonding. H-bond valences are from O–O distances for single H-bonds and calculated H–O distances for bifurcated H-bonds; estimated using Figs. 1 & 2 in Brown & Altermatt (1985). Bond-valence sums for OH groups in the "Σ+H" column is calculated such that valence sums to the H atoms are unity (cf.Table 8).

is lessened. A cosmetic disadvantage of refining against F_o^2 is that R indices based on F_o^2 are larger than for refinements based on $|F_o|$ using a threshold. In order to compare F_o^2 refinements with refinements based on $|F_o|$ with a $\sigma(F_o)$ threshold, the more conventional R index, based on $|F_o|$ values larger than $4\sigma(F_o)$, is also reported as R_1 in Table 2.

Description of the Structure

Cation coordination

There are eight symmetrically distinct U sites, all occupying the general position $4a$ in space group $P2_1ca$. These sites can be divided into two ordered sets, $U(1)$–$U(4)$ and $U(5)$–$U(8)$, that are pseudosymmetrically related by a 2-fold screw axis along [010] in the space group *Pbca* for the same unit cell. All U atoms are coordinated by seven anions in pentagonal dipyramidal arrangements (Fig. 1). Each $U\phi_7$ (ϕ: OH^- and O^{2-}) pentagonal dipyramid consists of two apical O^{2-} anions at distances in the range 1.74–1.83 Å and O–U–O angles in the range 172–179°, and five equatorial anions (O^{2-} and OH^-) in the range 2.17–2.78 Å (Table 4). A pentagonal arrangement of equatorial anions was predicted as the most stable configuration around a (UO_2) group by Evans (1963). The apical O^{2-} anions are designated as uranyl-O

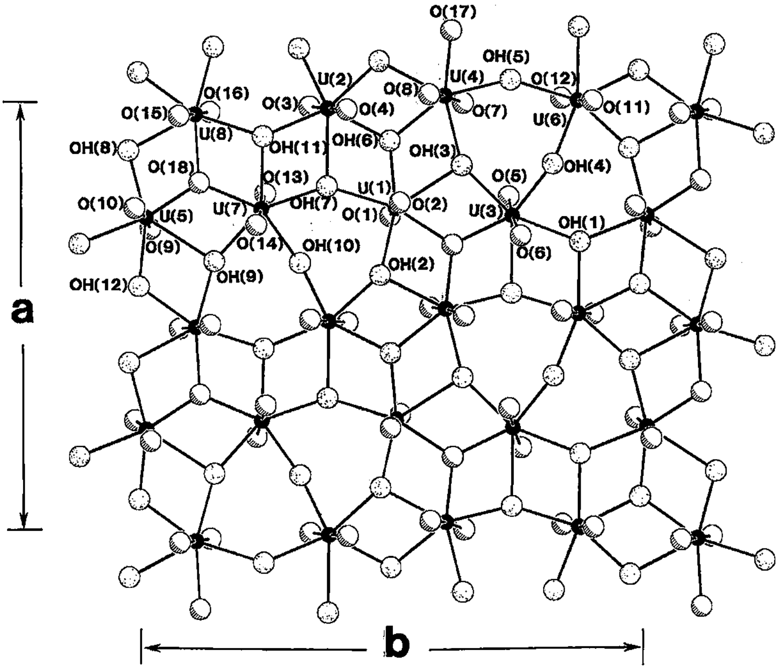

FIG. 1. Atomic arrangement in the structural sheet of schoepite. O atoms are shown as highlighted circles. OH groups are stippled, and small filled circles are U atoms. View along [001], $z \approx 0.75$.

atoms [O(uranyl)], and bond-valence calculations (Table 5) show that the U–O(uranyl) bonds have bond valences in the range 1.66 to 2.06 *vu* (valence units). The large difference in efficiencies in X-ray scattering of U and O makes the short U–O(uranyl) distances among the least accurately determined interatomic distances in the structures of uranyl compounds determined by X-ray diffraction. The U–O(uranyl) bond lengths determined for schoepite are comparable to those reported for other uranyl-oxy-hydroxide compounds (*e.g.*, Taylor 1971, Åberg 1978, Pagoaga *et al.* 1987). Bond-valence sums around the U atoms in schoepite (Table 5) are in the range 6.19–6.44 *vu*, significantly higher than the ideal value of 6.0 *vu*. This suggests that the U–O bond-valence parameters are somewhat in error, a factor that complicates the interpretation of hydrogen bonding in schoepite. However, if a U–O distance of 1.74 Å corresponds to a bond-valence of approximately 2.0 *vu*, longer distances (>1.74 Å) and lower bond-valences (<2.0 *vu*) may indicate O(uranyl) atoms that are acting as hydrogen-bond acceptors.

Structural unit

The $U\phi_7$ pentagonal dipyramids share edges to form dimers that further link by sharing edges to form staggered ribbons along [100] (Fig. 2); these ribbons then cross-link in the [010] direction by sharing edges and corners of the polyhedra. The result is a strongly bonded sheet of the form $[(UO_2)_8O_2(OH)_{12}]$ parallel to (001) (Fig. 2); this sheet constitutes the structural unit of schoepite, and the sheets stack along [001]. As the sheets are neutral, they are linked together by H-bonding only, through a complex network of H-bonding involving interlayer H_2O groups and O(uranyl) atoms and OH^- groups in the structural sheet. This explains the perfect {001} cleavage parallel to the sheets. Viewed along [001], the *U* sites are approximately superimposed, a feature of all uranyl oxide hydrate minerals (Pagoaga *et al.* 1987, Piret 1985, Piret *et al.* 1983, Piret-Meunier & Piret 1982, Mereiter 1979); there is no staggering of *U* sites perpendicular to the sheets, as for most high-temperature uranates (Loopstra & Rietveld 1969).

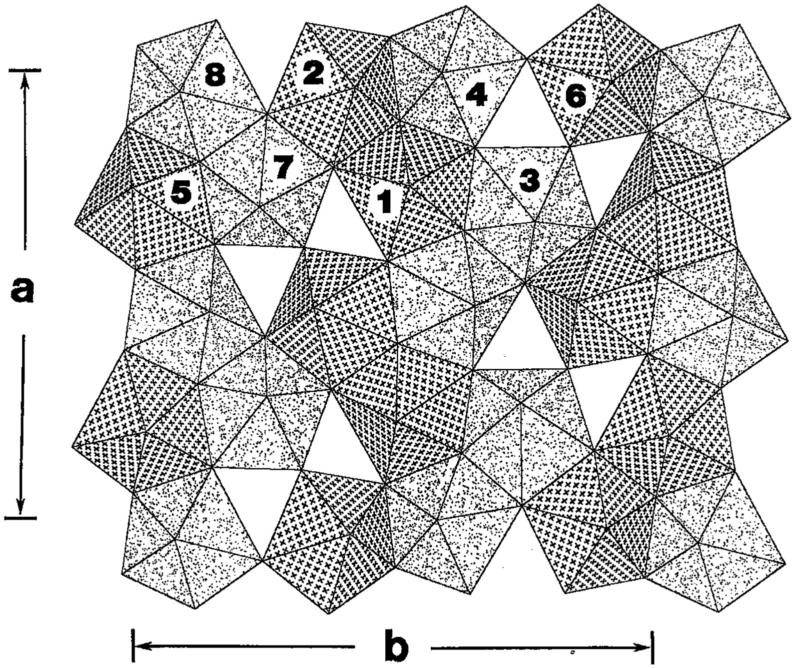

FIG. 2. Arrangement of $U\phi_7$ polyhedra in the structural sheet of schoepite. Different shadings of polyhedra show the two sets of polyhedra related by a pseudosymmetry axis, $^{[010]}2_1$. View along [001], $z \approx 0.75$. Labels refer to the U atom (*cf.* Fig. 1).

Interlayer H_2O groups

Twelve O atoms were located in the interlayer, none of which are directly bonded to any cation. Because the structural sheets are electrostatically neutral, all the interlayer O atoms must be H_2O groups and are designated as $W(1)...W(12)$. Ten of the twelve H_2O groups are located at the apices of two distorted pentagons, approximately 2.9 Å on edge; the remaining two H_2O groups are located between the pentagonal rings (Fig. 3). The H_2O groups that make up these pentagonal rings are not coplanar because of H-bonding interactions with the anions of the sheet. The pentagonal rings mimic the positions of the meridional anions in the $U(1)\phi_7$ and $U(5)\phi_7$ polyhedra (Fig. 4). The $U(5)\phi_7$ polyhedron is more distorted than the $U(1)\phi_7$ polyhedron, and the pentagonal ring associated with the $U(5)\phi_7$ polyhedron is the more distorted of the two (Fig. 3). Each pentagonal ring of H_2O groups circumscribes O(uranyl) atoms from the $U(1)$ and $U(5)$ polyhedra in the two adjacent sheets; each is buckled, such that two of the five H_2O groups are closer to one adjacent structural sheet, and three of the H_2O groups are closer to the other structural sheet. There is no evidence for disorder or partial occupancy of the interlayer *W* sites.

Pseudo-symmetry

The arrangement of U atoms, O(sheet) atoms and interlayer H_2O groups is strongly pseudo-centrosymmetrical. Only the O(uranyl) atoms are not pseudo-centrosymmetrical, and their positions about the U atoms are largely responsible for the lack of a center of symmetry. The combined effects of H-bonding and steric crowding by adjacent O(sheet) atoms and interlayer H_2O groups cause the O(uranyl) atoms to deviate significantly from a centro-symmetrical arrangement in schoepite.

Chemical composition of schoepite

The structure solution shows the structural formula of schoepite to be $[(UO_2)_8O_2(OH)_{12}](H_2O)_{12}$, corre-

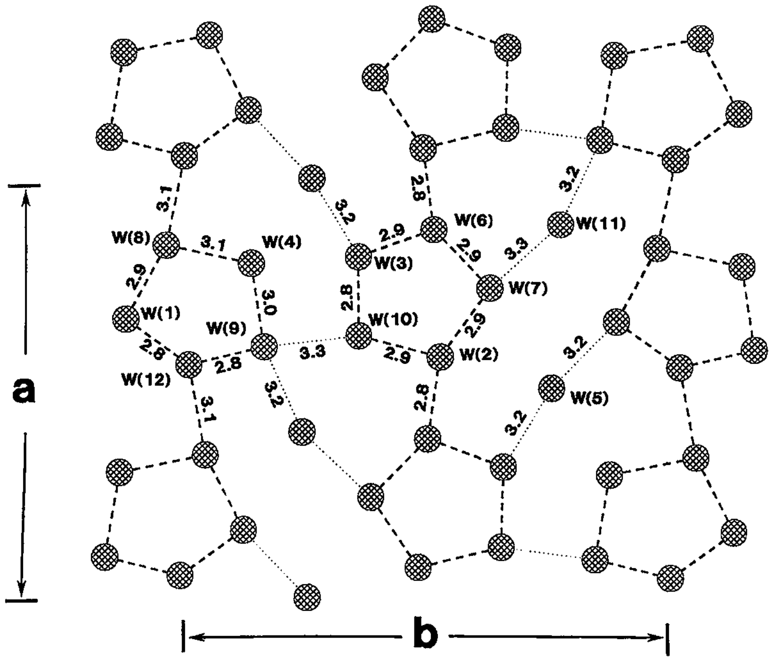

FIG. 3. Atomic arrangement of interlayer H_2O groups in schoepite, with possible intrasheet H-bonds indicated as dashed lines (≤3.1 Å). Interatomic distances greater than 3.1 Å but less than 3.4 Å are shown as dotted lines. View along [001], $z \approx 0.5$.

sponding to the composition $UO_3{\cdot}2.25H_2O$, in good agreement with that originally determined by Billiet & de Jong (1935) from the measured density and unit-cell parameters. The composition commonly reported for schoepite is $UO_3{\cdot}2H_2O$. It was determined by thermogravimetric analysis (TGA) on both natural (Protas 1959) and synthetic material (Bignand 1955, Peters 1967). Our results indicate that the name "synthetic schoepite" for the compound $UO_3{\cdot}2H_2O$ may not be appropriate.

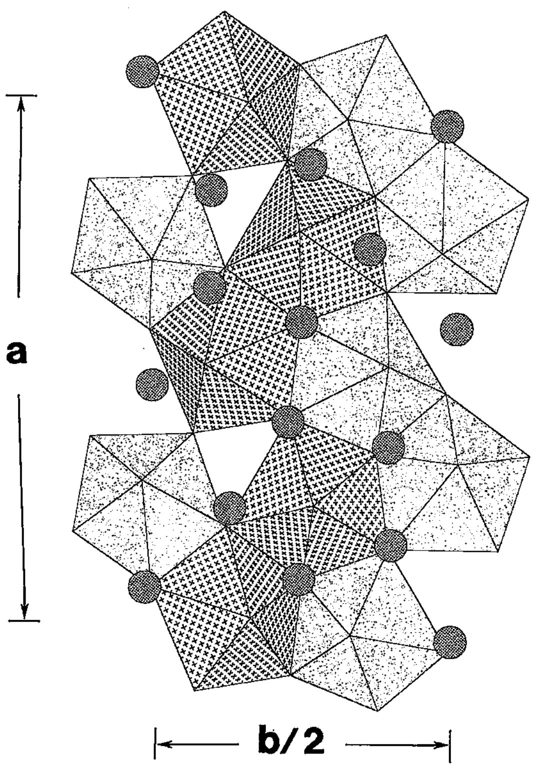

FIG. 4. The arrangement of interlayer H_2O groups (hatched circles) relative to the $U\phi_7$ polyhedra of the adjacent structural unit. Two of the more regular pentagonal rings are shown (center) with six H_2O groups that are not members of the rings [W(5) and W(11)]: note that half of the H_2O groups overlay anion positions in the adjacent sheet. The other half of the H_2O groups not in registry with the anions of the sheet match up with the anions of the other adjacent sheet (not shown in this view). The shading of the polyhedra is the same as for Figure 2. View along [001], $z \approx 0.375$.

Hydrogen Bonding in Schoepite

It is usually not possible to locate H atoms directly from X-ray diffraction data by structure refinement and difference-Fourier maps for such highly absorbing material as the uranium oxy-hydroxy-hydrate minerals. For schoepite in particular, this is unfortunate because the chemical composition and perfect {001} cleavage indicate that H bonding must be the mechanism whereby the sheets of the structural unit are linked. Furthermore, the similar physical and crystallographic properties of schoepite and metaschoepite (Christ & Clark 1960, Debets & Loopstra 1963) suggest that these structures are distinguished primarily by differences in their arrangements of interlayer H-bonding. Despite these problems, we can get some idea of the interlayer H-bonding in schoepite from the locations of the O atoms of the H_2O groups and from the stereochemical characteristics of H_2O groups and their associated networks of H bonds (Hawthorne 1992, 1994).

Geometrical characteristics

Figure 4 shows the arrangement of H_2O groups relative to the adjacent polyhedra of the structural unit. Some of the H_2O groups map out the peripheral vertices of the underlying $U\phi_7$ polyhedra, whereas other H_2O groups do not show this correspondence; the latter groups map out the peripheral vertices of the overlying polyhedra. The H_2O groups form a slightly puckered sheet parallel to {001}. There is a cooperative puckering between the sheet of the structural unit and the interlayer sheet of H_2O groups, such that all H_2O groups lie between 2.5 and 2.9 Å from OH groups of the structural unit. These short distances must represent H bonds linking the structural sheets to the interlayer H_2O groups. Within the H_2O sheet, adjacent H_2O groups are separated by distances of 2.8 to 3.4 Å (Fig. 3). The shorter distances represent H-bonds within the H_2O sheet. Some constraints on the bonding interactions within the H_2O sheet can be inferred by examining the stereochemical characteristics of the H_2O groups themselves.

H-bond interactions between the H_2O layer and the structural unit

There are twelve symmetrically distinct H_2O groups and twelve symmetrically distinct OH groups per formula unit. Thus there are thirty-six D–H (donor – hydrogen) and thirty-six (equivalent) H...A^* (hydrogen...acceptor) bonds (A^* is used here to emphasize that, in the case of bifurcated bonds, each H...A interaction contributes one-half to A^*). As each H atom is involved in an equal number of D–H and H...A^* bonds, there must be an equal number of D–H and H...A^* bonds both within the H_2O sheet and between the H_2O sheet and the structural unit. This can only be true if half the structural-unit – H_2O interactions are of the D–H...A^* type and the other half are of the A^*...H–D type. In other words, the total bond-valence contribution to the H_2O sheet must be balanced by an equal bond-valence contribution *from* the H_2O sheet to the structural unit. The positioning of the H_2O groups relative to the OH groups (Figs. 5, 6) suggests that there must be an H-bonding interaction between each OH group and its opposing H_2O group. Each of the twelve OH groups in the structural unit acts as a donor to a nearby H_2O group, and these twelve H-bonds from the structural unit to the H_2O sheet must be balanced by twelve H-bonds ($D \rightarrow A^*$) from the H_2O sheet to the structural unit. This conclusion is in accord with observed U–O(uranyl) distances, and suggests that O(uranyl) atoms act as acceptor anions for H bonds from the H_2O groups of the interlayer sheet.

As the coordination of each O atom in an H_2O group is expected to be approximately tetrahedral, several O atoms in the structural unit can be eliminated from consideration as H-bond acceptors. First, the two O(sheet) atoms O(17) and O(18) cannot act as acceptors because these atoms are not displaced toward the H_2O sheet and are well shielded from H-bonding interactions by surrounding O(uranyl) atoms. Second, four O(uranyl) atoms are doubtful acceptors, as they occupy positions inside the five-membered H_2O rings, and are therefore not stereochemically suited to accept H-bonds from the H_2O groups of these rings; these are the four O(uranyl) atoms bonded to U(1) and U(5), respectively O(1), O(2), O(9) and O(10) (Fig. 1). Eliminating these six O atoms from consideration leaves twelve O(uranyl) atoms in the structural unit as potential H-bond acceptors.

Isolated H_2O groups

Two H_2O groups, W(5) and W(11), are not members of the pentagonal rings (Fig. 3), and cannot be tetrahedrally coordinated. These two H_2O groups act as acceptors only for the adjacent OH groups in the structural unit, OH(5) and OH(11), respectively, and are donors to nearby O(uranyl) atoms. W(5) acts as a donor to O(3) and O(16). W(11) acts as a donor to two of the three O(uranyl) atoms, O(5), O(7) and O(12). Which two of the three act as acceptors cannot be ascertained, as all three seem equally likely. The W(11) H-bonds may be disordered or bifurcated (or both), with three arrangements possible in each case. The H-bonding interactions between W(11) and its associated O(uranyl) atoms are weak, distances being on the order of 3.0 to 3.2 Å (Table 6). Thus W(5) and W(11) account for four of the twelve H-bonds that emanate from the H_2O sheet to the structural unit, leaving eight H-bonds to be assigned.

Figure 5 illustrates the structural role that W(5) and

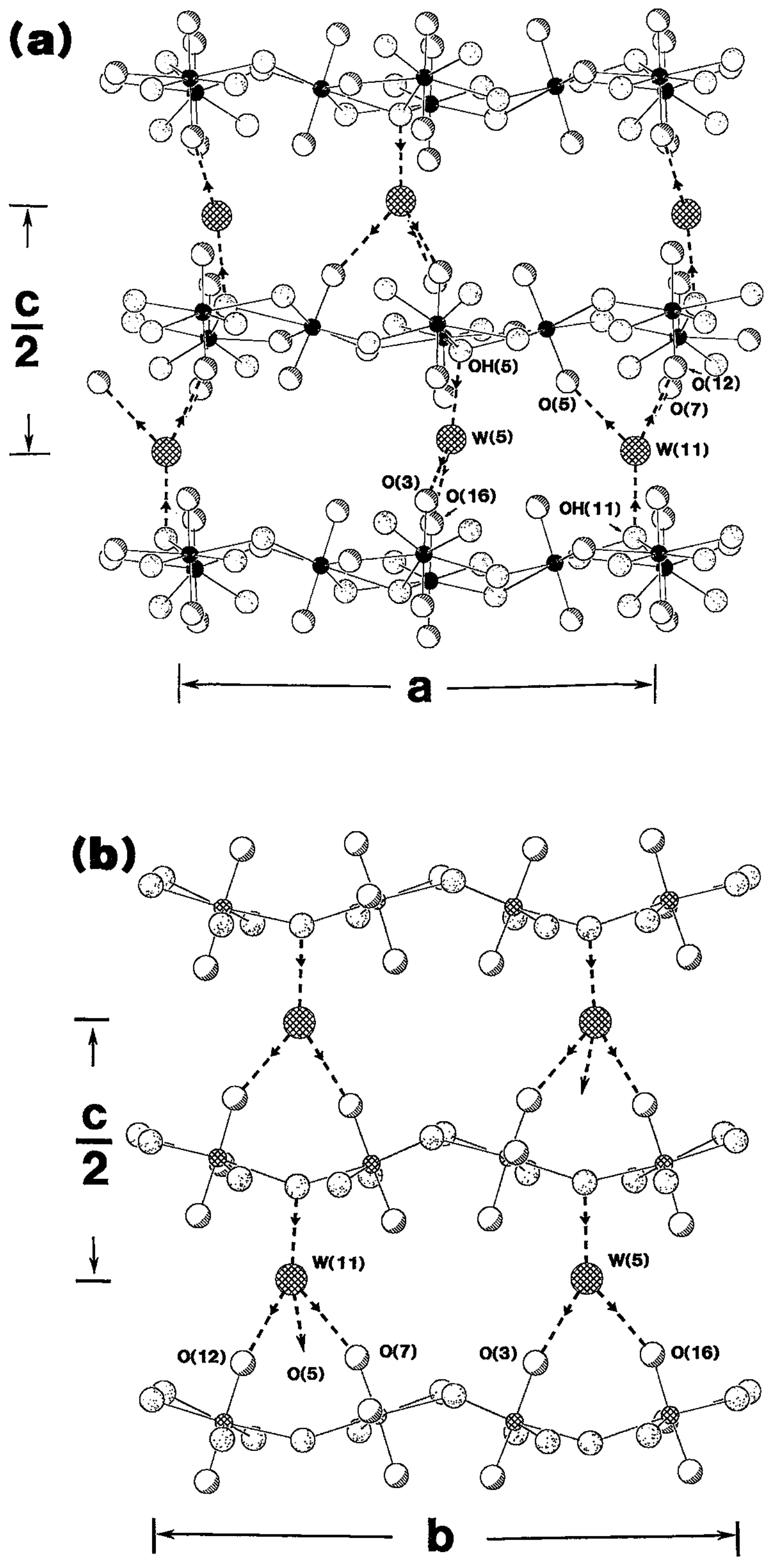

FIG. 5. H-bond interactions between the structural unit and the two H_2O groups that are not members of the pentagonal rings, W(5) and W(11). W(11) is shown with all three possible $D \rightarrow A$ interactions; see text. H_2O groups are shown as hatched circles; other shadings as for Figure 1. (a) View along [010], $y \approx 0.75$; (b) View along [$\bar{1}$00], $x \approx 0.25$. O(5) is behind the plane of the illustration, and the W(11) $\rightarrow$ O(5) bond is shown as an arrow.

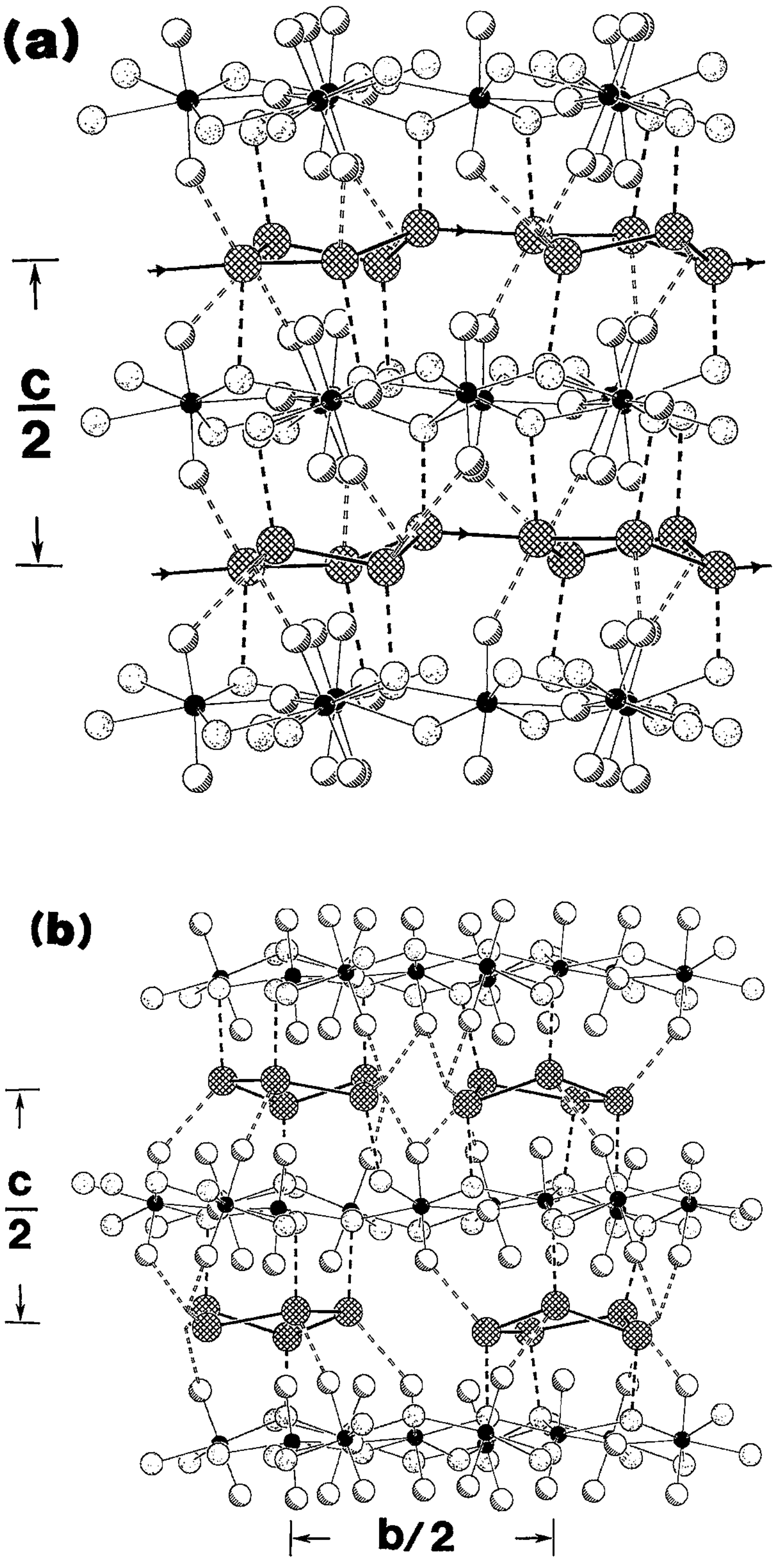

FIG. 6. H-bond interactions between the structural unit and the pentagonal rings of the H_2O sheet. Intrasheet H-bonds between H_2O groups are shown as heavy solid lines. $D \rightarrow A$ interactions from OH groups in the structural unit to H_2O groups are shown as heavy dashed lines. $D \rightarrow A$ interactions from H_2O groups to O(uranyl) atoms in the structural unit are shown as double dashed lines. Bifurcated H-bonds are shown emanating from inferred H positions for W(3), W(4), W(9) and W(10). W(5) and W(11) are omitted. Shadings and bonds as for Figure 5. (a) View along [010], $y \approx 0.5$, showing the more regular of the two pentagonal rings and the associated H-bonds; the H-bond arrangement for the more distorted pentagonal ring is similar. (b) View along [100], $x \approx 0.25$, showing the arrangement of the two pentagonal rings and the H-bonding interactions between them due to the bifurcated H-bonds (see text).

TABLE 6. POSSIBLE H-BONDS (Å) FOR INTERLAYER H_2O IN SCHOEPITE (<3.3 Å)

W(1)←OH(1)	2.68(3)	W(7)←OH(7)	2.94(3)
W(1)–W(12)	2.80(3)	W(7)–W(6)	2.89(3)
W(1)–W(8)	2.87(3)	W(7)–W(2)	2.90(3)
W(1)→O(14)u*	2.98(3)	W(7)→O(5)u	3.05(3)
W(2)←OH(2)	2.81(3)	W(8)←OH(8)	2.74(3)
W(2)←W(6)	2.83(2)	W(8)–W(12)	3.14(3)
W(2)–W(7)	2.90(2)	W(8)–W(1)	2.87(3)
W(2)–W(10)	2.94(3)	W(8)–W(4)	3.05(3)
W(2)→O(8)u	2.77(3)	W(8)→O(15)	2.86(3)
W(3)←OH(3)	2.89(3)	W(9)←OH(9)	2.66(3)
W(3)–W(10)	2.77(3)	W(9)–W(4)	2.98(3)
W(3)–W(6)	2.89(2)	W(9)–W(12)	2.81(3)
W(3)→O(3)u	3.31(3)	W(9)→O(12)u	3.13(3)
W(3)→O(13)u	2.97(3)	W(9)→O(6)u	2.96(3)
W(4)←OH(4)	2.90(3)	W(10)←OH(10)	2.78(3)
W(4)–W(9)	2.98(3)	W(10)–W(3)	2.77(3)
W(4)–W(8)	3.05(3)	W(10)–W(2)	2.94(3)
W(4)→O(13)u	3.08(3)	W(10)→O(6)u	3.03(3)
W(4)→O(16)u	3.11(3)	W(10)→O(7)u	3.18(3)
W(5)←OH(5)	2.78(3)	W(11)←OH(11)	2.67(3)
W(5)→O(16)u	2.95(3)	W(11)→O(7)u	3.12(3)
W(5)→O(3)u	2.88(3)	W(11)→O(12)u	3.02(3)
		W(11)→O(5)u	3.06(3)
W(6)←OH(6)	2.50(2)	W(12)←OH(12)	2.74(2)
W(6)→W(2)	2.83(2)	W(12)–W(8)	3.14(3)
W(6)–W(3)	2.89(2)	W(12)–W(9)	2.81(3)
W(6)–W(7)	2.89(3)	W(12)–W(1)	2.80(2)
		W(12)→O(11)	3.05(3)

* u = uranyl oxygen atom.
Arrows indicate inferred D→A relationships.

W(11) play in the schoepite structure. The uranyl ions to which these two H_2O groups are H-bonded are displaced quite noticeably toward W(5) and W(11). The combined effects of the short OH–H_2O bonds and the tilting of the uranyl ions result in significant puckering of the structural sheet, especially along [010] (Fig. 5b).

Pentagonal rings

The ten remaining H_2O groups are all members of the pentagonal rings (Fig. 3). Three of these, W(1), W(2) and W(7), must act as H-bond donors to O(uranyl) atoms O(14), O(8) and O(5), respectively, as these O(uranyl) atoms occupy positions that complete the tetrahedral coordination around the O atoms of these three H_2O groups. Also, O(14), O(8) and O(5) have relatively long bonds (>1.75 Å) to their associated U atoms (Table 4).

Four H_2O groups, W(3), W(4), W(9) and W(10), cannot donate H bonds to single O(uranyl) atoms, as there are no O(uranyl) atoms in the appropriate positions. The four H-bonds emanating from these four H_2O groups to the structural unit are bifurcated, with the H atoms lying approximately midway between two O(uranyl) acceptors. These donor–acceptor trios are: W(3)–H...O(3) and O13; W(4)–H...O(13) and O(16); W(9)–H...O(6) and O(12); W(10)–H...O(6) and O(7). Thus we have accounted for eleven of the twelve required H bonds emanating from the H_2O sheet to the structural unit, one each from W(1), W(2), W(3), W(4), W(7), W(9) and W(10), and two each from W(5) and W(11).

The twelfth H bond is somewhat problematic. At least one of the three H_2O groups, W(6), W(8) and W(12), must act as an H-bond donor to the structural unit. Each of these three H_2O groups occupies a position adjacent to a neighboring H_2O ring (Fig. 3). O(15) completes the tetrahedral environment about W(8) but, despite the W(8)–O(15) distance (2.86 Å), the short O(15)–U(8) bond length (1.74 Å) casts doubt on a strong H-bond interaction between W(8) and O(15). Another likely H-bond acceptor is O(11), with a bond distance of 1.80 Å to U(6); however, O(11) is 3.0 Å from W(12) and is not in an optimal position with regard to the expected tetrahedral environment of W(12). Thus W(12)–O(11) represents a weak H-bond interaction. This ambiguity in the position of this last H-bond cannot be resolved, and H-bonds from W(8) and W(12) may both be bifurcated. Figure 6 shows the proposed H-bonding interactions between the two interlayer H_2O rings and the structural unit.

To restate the role of the O(uranyl) atoms as H-bond acceptors, the O(uranyl) atoms, O(8), O(11) and O(14), act as acceptors for one H_2O group each. O(uranyl) atoms O(3), O(5), O(6), O(7), O(12), O(13) and O(16) act as acceptors for two H_2O groups each. The six O(uranyl) atoms, O(1), O(2), O(4), O(9), O(10) do not act as H-bond acceptors; the role of O(15) is uncertain. Ten of the twelve H_2O groups act as H-bond donors to the structural unit, with W(6) acting as a donor only to other H_2O groups within the H_2O sheet.

H-bond interactions within the H_2O layer

No unique solution to the H-bonding arrangement between adjacent H_2O groups can be derived, although donor–acceptor relationships within the H_2O sheet can be constrained by the H_2O–O(uranyl) atom arrangements discussed above. Within each pentagonal ring, all five H-bonds must have the same directional (or rotational) sense. For each ring, two rotational senses can be defined; viewed down [001], these are "clockwise" (C) and "anticlockwise" (A). Thus four combinations are possible for the two symmetrically distinct pentagonal rings: C–C, A–A, C–A and A–C, all of which are compatible with the H-bonding interactions between the H_2O sheet and the structural unit as described above. The H-bond interactions between the pentagonal rings are more limited. W(6), which does not act as a donor to an O(uranyl) atom, must donate to W(2) in the next pentagonal ring, and W(8) may donate to W(12) in the neighboring ring.

TABLE 7. ANGLES AROUND INTERLAYER H_2O GROUPS IN SCHOEPITE

OH(1)-W(1)-W(12)	102.9(8)°	OH(7)-W(7)-W(6)	100.0(8)°	OH(4)-W(4)-W(9)	108.8(9)°	OH(10)-W(10)-W(3)	109.8(10)°
OH(1)-W(1)-W(8)	94.8(8)°	OH(7)-W(7)-W(2)	98.7(7)°	OH(4)-W(4)-W(8)	112.2(9)°	OH(10)-W(10)-W(2)	108.6(9)°
OH(1)-W(1)-O(14)	141.5(9)°	OH(7)-W(7)-O(5)	135.0(9)°	OH(4)-W(4)-O(13)	124.8(8)°	OH(10)-W(10)-O(6)	129.4(9)°
W(12)-W(1)-W(8)	97.2(8)°	W(6)-W(7)-W(2)	100.9(7)°	OH(4)-W(4)-O(16)	124.3(9)°	OH(10)-W(10)-O(7)	125.6(10)°
W(12)-W(1)-O(14)	109.4(9)°	W(6)-W(7)-O(5)	102.0(8)°	W(9)-W(4)-W(8)	107.4(9)°	W(3)-W(10)-W(2)	102.5(8)°
W(8)-W(1)-O(14)	101.3(8)°	W(2)-W(7)-O(5)	114.8(8)°	W(9)-W(4)-O(13)	64.1(8)°	W(3)-W(10)-O(6)	71.3(7)°
				W(9)-W(4)-O(16)	120.5(9)°	W(3)-W(10)-O(7)	123.1(10)°
OH(2)-W(2)-W(6)	83.4(8)°	OH(8)-W(8)-W(12)	78.8(8)°	W(8)-W(4)-O(13)	122.2(10)°	W(2)-W(10)-O(6)	120.7(9)°
OH(2)-W(2)-W(7)	93.0(8)°	OH(8)-W(8)-W(1)	99.6(9)°	W(8)-W(4)-O(16)	77.3(7)°	W(2)-W(10)-O(7)	73.2(7)°
OH(2)-W(2)-W(10)	100.5(8)°	OH(8)-W(8)-W(4)	94.7(8)°	O(13)-W(4)-O(16)	64.5(7)°	O(6)-W(10)-O(7)	64.6(7)°
OH(2)-W(2)-O(8)	142.3(8)°	OH(8)-W(8)-O(15)	141.7(10)°				
W(6)-W(2)-W(7)	152.9(7)°	W(12)-W(8)-W(1)	162.7(8)°	OH(5)-W(5)-O(16)	140.4(8)°	OH(11)-W(11)-O(7)	132.9(10)°
W(6)-W(2)-W(10)	96.8(7)°	W(12)-W(8)-W(4)	91.2(7)°	OH(5)-W(5)-O(3)	146.9(9)°	OH(11)-W(11)-O(12)	145.3(10)°
W(6)-W(2)-O(8)	70.3(7)°	W(12)-W(8)-O(15)	65.4(7)°	O(16)-W(5)-O(3)	70.1(7)°	O(12)-W(11)-O(7)	65.1(8)°
W(7)-W(2)-W(10)	110.2(8)°	W(1)-W(8)-W(4)	106.1(8)°			O(5)-W(11)-O(12)	75.9(8)°
W(7)-W(2)-O(8)	98.4(7)°	W(1)-W(8)-O(15)	110.4(10)°			O(5)-W(11)-O(7)	68.4(8)°
W(10)-W(2)-O(8)	108.8(8)°	W(4)-W(8)-O(15)	99.2(9)°			OH(11)-W(11)-O(5)	135.2(9)°
OH(3)-W(3)-W(10)	104.3(8)°	OH(9)-W(9)-W(4)	101.4(10)°	OH(6)-W(6)-W(2)	93.4(8)°	OH(12)-W(12)-W(8)	90.0(8)°
OH(3)-W(3)-W(6)	104.9(8)°	OH(9)-W(9)-W(12)	106.1(10)°	OH(6)-W(6)-W(3)	106.7(8)°	OH(12)-W(12)-W(9)	112.0(9)°
OH(3)-W(3)-O(3)	137.9(7)°	OH(9)-W(9)-O(12)	147.8(10)°	OH(6)-W(6)-W(7)	106.4(9)°	OH(12)-W(12)-W(1)	107.6(8)°
OH(3)-W(3)-O(13)	145.0(8)°	OH(9)-W(9)-O(6)	150.1(10)°	W(2)-W(6)-W(3)	100.4(7)°	W(8)-W(12)-W(9)	91.5(7)°
W(10)-W(3)-W(6)	104.3(8)°	W(4)-W(9)-W(12)	89.8(8)°	W(2)-W(6)-W(7)	139.4(8)°	W(1)-W(12)-W(8)	132.7(8)°
W(10)-W(3)-O(3)	117.9(9)°	W(4)-W(9)-O(12)	109.2(10)°	W(3)-W(6)-W(7)	106.8(8)°	W(1)-W(12)-W(9)	119.4(9)°
W(10)-W(3)-O(13)	65.7(7)°	W(4)-W(9)-O(6)	66.0(7)°			W(1)-W(12)-O(11)	64.3(6)°
W(6)-W(3)-O(3)	66.6(6)°	W(12)-W(9)-O(12)	65.1(7)°			OH(12)-W(12)-O(11)	134.2(8)°
W(6)-W(3)-O(13)	110.0(9)°	W(12)-W(9)-O(6)	101.1(10)°			W(9)-W(12)-O(11)	110.2(9)°
O(3)-W(3)-O(13)	62.1(7)°	O(6)-W(9)-O(12)	57.4(7)°			W(8)-W(12)-O(11)	72.0(7)°

The two H_2O groups, W(2) and W(12), each act as an acceptor for three adjacent H_2O groups, rather than the two expected to complete a tetrahedral environment. The pseudo-centrosymmetrical relationship among the O atoms involved in H-bonding is evident in Figure 7 [an approximate center of symmetry is located at the center of the figure, between O(6) and O(13)]; however, the inferred H-bonding interactions violate *Pbca* symmetry. This suggests that it is the pattern of H-bonding in schoepite that is primarily responsible for the reduction in the symmetry from *Pbca* to $P2_1ca$, as it displaces the O(uranyl) atoms from their ideal positions in *Pbca*.

The H-bond contributions to the O(uranyl) atoms are added to the bond-valence sums in Table 5, and the estimated bond-valence for interlayer H_2O groups are given in Table 8. These H-bond contributions are estimates, but they indicate that the H-bonding arrangement proposed for schoepite is reasonable.

Comparison with Related Structures

The twenty-one known uranyl oxide hydrates display close structural similarities to schoepite (Burns *et al.* 1996, Baran 1992, Čejka & Urbanec 1990, Smith 1984, Deliens 1977b, Sobry 1973, Peters 1967, Protas 1959). The uranyl oxide hydrates are all sheet structures with one perfect cleavage. Crystals are optically negative, with similar X-ray powder-diffraction patterns, and they commonly have pseudohexagonal habits. Their unit cells can be described in terms of a primitive pseudohexagonal cell (Deliens 1977b, Christ & Clark 1960): $a_{hex} \approx 4.1$, $c_{hex} \approx 7.0$ to 7.5 Å, $\gamma \approx 120°$. A reduced *C*-centered orthorhombic subcell (a_{ro}, b_{ro}, c_{ro}) can also be defined from the primitive pseudohexagonal cell (compare with Pagoaga 1983):

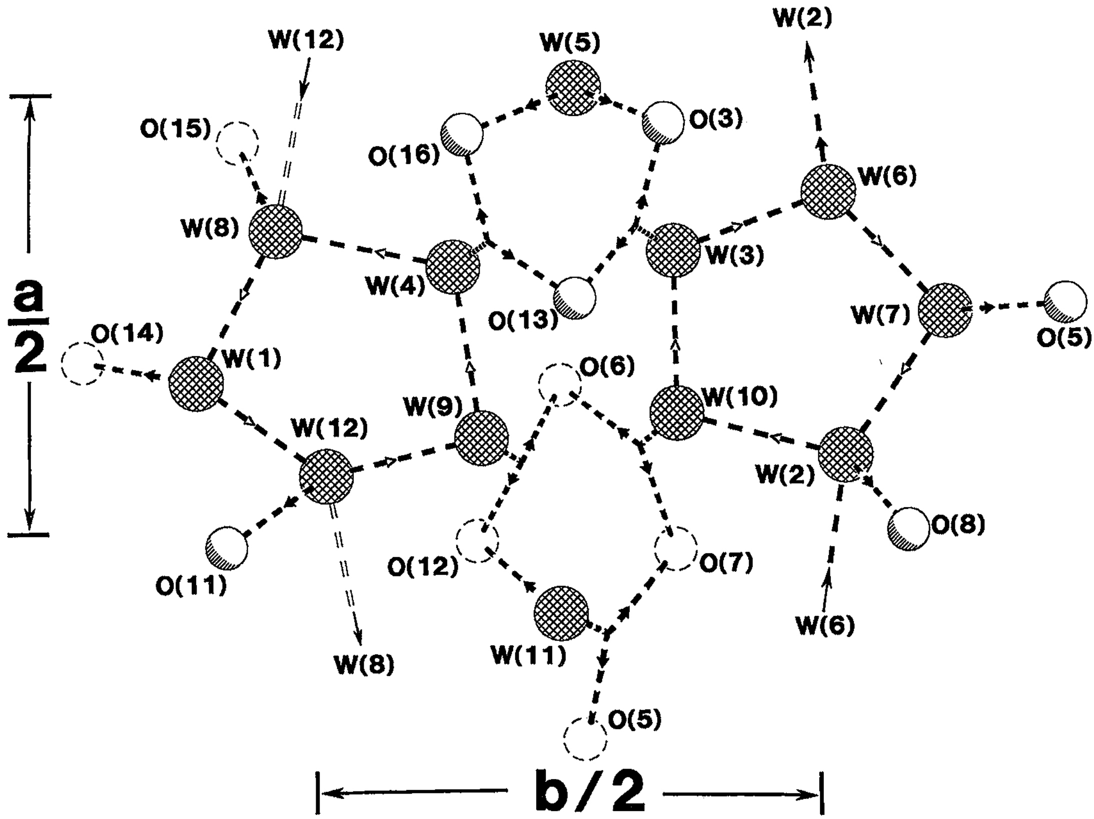

FIG. 7. View down [001] showing the H-bond interactions among the H_2O groups and between H_2O groups and the O(uranyl) atoms that act as H-bond acceptors. The H_2O groups are hatched circles at $z \approx 0.5$. O(uranyl) atoms above the H_2O sheet are shown as highlighted circles; O(uranyl) atoms below the H_2O sheet are shown as dashed circles. Arrows indicate inferred $D \rightarrow A$ interactions; hollow arrows indicate ambiguous intrasheet H-bonds. The H-bonding interactions for W(8) and W(12) are uncertain. One of three possible bifurcated H-bond arrangements is shown for W(11). The rotational sense of the intrasheet H-bonds shown is "A–C", one of four possible arrangements (see Table 6 and text for discussion).

$$a_{ro} \approx (2 \cdot a_{hex}) \cdot \sin(120°) \approx 7.0 \text{ Å}$$
$$b_{ro} = a_{hex} \approx 4.1 \text{ Å}$$
$$c_{ro} = c_{hex} \approx 7.0 \text{ to } 7.5 \text{ Å } (\textit{layer spacing})$$

The unit cells of most uranyl oxide hydrates are integral multiples of this reduced orthorhombic subcell. Most fall into one of two groups: (1) those for which $b = n2b_{ro}$; (2) those for which $b = n3b_{ro}$ (n is an integer, usually 1 or 2). Schoepite and the two uranyl oxide hydrate minerals containing Pb, fourmarierite and curite, fall into the first group; for schoepite, $a_s = 2a_{ro}$, $b_s = 4b_{ro}$, $c_s = 2c_{ro}$. The uranyl oxide hydrates containing alkaline earths, such as becquerelite, billietite, compreignacite, protasite and wölsendorfite, fall into the (larger) second group. Other uranyl oxide hydrates are known with unit-cell parameters that are not simple multiples of the reduced orthorhombic subcell; however, these structures can also be represented in this way by redefining their unit cells such that the structural sheets are parallel to $(001)_{ro}$ (Miller *et al.* 1996).

Fourmarierite

The structure of schoepite is strikingly similar to that of fourmarierite, $Pb[(UO_2)_4O_3(OH)_4] \cdot 4H_2O$ (Piret 1985); cell parameters are similar, and the structural sheet in schoepite is topologically identical to that in fourmarierite (Figs. 2, 8). Schoepite and fourmarierite are the only two minerals known with this type of sheet arrangement (Burns *et al.* 1996). If two of the OH groups in schoepite [OH(6) and OH(12)] are replaced by O^{2-}, the composition of the sheet changes to that of fourmarierite. The negative charge on the

TABLE 8. ESTIMATED BOND-VALENCE SUMS TO INTERLAYER H_2O GROUPS *

	W–H⁻A (*vu*)	D⁻*W* (*vu*)	Σ (*vu*)
W(1)	*W*(12): 0.82; O(14) 0.89	OH(1): 0.21; *W*(8): 0.16	2.08
W(2)	*W*(10): 0.87; O(8): 0.81	OH(2): 0.17; *W*(6): 0.17; *W*(7): 0.15	2.17
W(3)	*W*(6): 0.84; ‡(b): 0.80	OH(3): 0.15; *W*(10): 0.19	1.98
W(4)	*W*(8): 0.92; (b): 0.80	OH(4): 0.15; *W*(9): 0.11	1.98
W(5)	O(3): 0.84; O(16): 0.87	OH(5): 0.18	1.89
W(6)	*W*(2): 0.83; *W*(7): 0.84	OH(6): 0.36; *W*(3):0.16	2.19
W(7)	*W*(2): 0.85; O(5):0.93	OH(7): 0.13; *W*(6):0.16	2.07
W(8)	*W*(1): 0.84; O(15): 0.84	OH(8): 0.19; *W*(4):0.08; *W*(12): 0.03†	1.98
W(9)	*W*(4): 0.89; (b): 0.80	OH(9): 0.22; *W*(12): 0.18	2.09
W(10)	*W*(3): 0.81; (b): 0.80	OH(10): 0.19; *W*(2): 0.13	1.93
W(11)	O(12): 0.91; (b): 0.80	OH(11): 0.22	1.93
W(12)	*W*(9): 0.82; (b): 0.80†	OH(12): 0.20; *W*(1): 0.18	2.00

* Estimated using Fig. 2 in Brown & Altermatt (1985). Bifurcated H-bonds contribute 0.8 *vu* to the donor H_2O group, all other *W*–H contributions calculated such that valence sums to the H atoms are unity (cf. Table 5). Intra-layer H-bonds from *W*–*W* distances (Table 6) and the H-bonding shown in Fig. 7.
‡ (b) indicates bifurcated bonds (cf. Table 6, Fig. 7).
† Bond-valence estimates for bifurcated H-bonds from W(12) to O(11) & W(8) and from W(11) to O(5) & O(7).

structural sheet in fourmarierite is compensated by interlayer Pb^{2+} cations. Fourmarierite contains eight interlayer H_2O groups as compared to twelve in schoepite. Four H_2O groups are bonded to two Pb atoms, forming $[Pb_2(H_2O)_4]^{4+}$ dimeric groups. Each $[Pb_2(H_2O)_4]^{4+}$ dimer in fourmarierite replaces eight H_2O groups in the schoepite interlayer. The remaining four H_2O groups in fourmarierite occupy interlayer sites similar to the *W* sites in schoepite.

Becquerelite, billietite and protasite

The three protasite-group minerals, becquerelite, $Ca[(UO_2)_6O_4(OH)_6]{\cdot}8H_2O$, billietite, $Ba[(UO_2)_6O_4(OH)_6]{\cdot}4–8H_2O$, and protasite, $Ba[(UO_2)_3O_3(OH)_2]{\cdot}3H_2O$, are structurally related (Pagoaga *et al.* 1987). Although they display many similarities to the structures of schoepite and fourmarierite, the structural sheets in the minerals of the protasite group are significantly different from those (Fig. 8). Schoepite and fourmarierite have corner-sharing $U\phi_7$ polyhedra, whereas the protasite-group minerals have only edge-sharing $U\phi_7$ polyhedra (Pagoaga *et al.* 1987). As a result, the triangular "holes" in the structure sheets of the protasite-group minerals are isolated rather than forming the "bow tie" dimers in schoepite and fourmarierite (Fig. 8). This difference in the two types of structural sheet is the main structural distinction between the minerals of the protasite and fourmarierite groups (Miller *et al.* 1996).

These two types of structural sheet can be readily distinguished on the basis of unit-cell parameters. The *a*–*b* plane is parallel to the structural sheets, and *a* is $n \times (\sim 7$ Å) for both types of sheet. However, *b* is $n \times (\sim 6.15$ Å) for the protasite group, but is $n \times (\sim 8.2$ Å) in schoepite and fourmarierite (compare the reduced cells of Pagoaga 1983). For the known structures of both groups, $n = 2$ along *b*. The reason for the different *b* dimensions can be understood by noting that the ratio of uranyl ions to O(sheet) atoms differs for the two types of structural sheet. For the protasite-

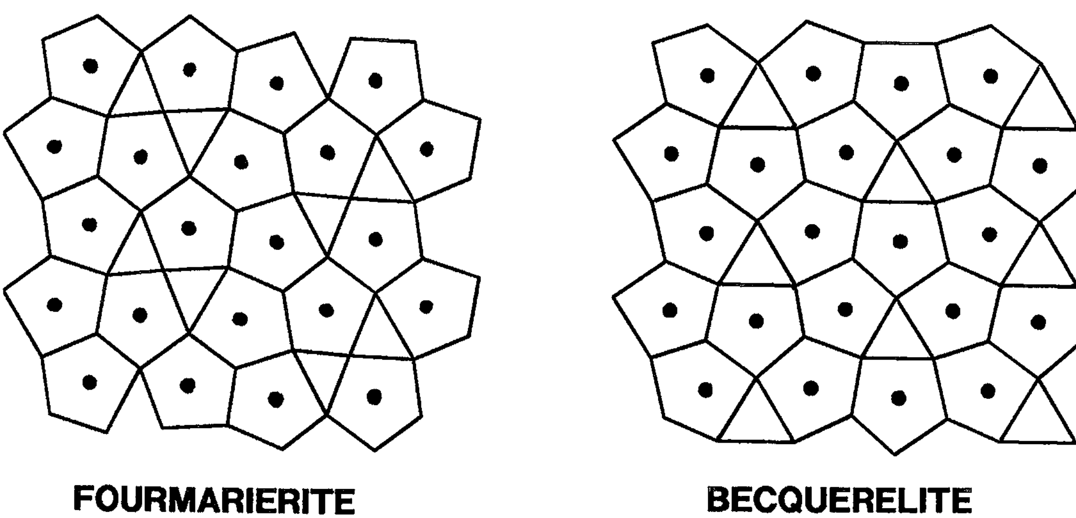

FIG. 8. Outlined $U\phi_7$ polyhedra in the structural units of fourmarierite, $Pb[(UO_2)_4O_3(OH)_4]{\cdot}4H_2O$, and becquerelite, $Ca[(UO_2)_6O_4(OH)_6]{\cdot}8H_2O$. The two sheet types are distinguished by the different arrangements of triangular holes, which are paired in fourmarierite ("bow ties"), and isolated in becquerelite. Fourmarierite has the same arrangement of polyhedra as schoepite. U atoms are indicated by filled circles; O(uranyl) atoms are omitted.

group minerals, this ratio is 3:5; for schoepite and fourmarierite, it is 4:7. Thus one additional O(sheet) atom is required for every twelve uranyl ions in the fourmarierite-type sheet as compared to the protasite-type sheet. The additional ~2.05 Å every ~8.15 Å along *b* is therefore required to accommodate the additional [2]-coordinated O(sheet) atoms in schoepite and fourmarierite.

There are no known uranyl oxide hydrate structures based on a hybrid of the two types of sheet. However, this could occur by means of stacking disorder along *b*. This may explain some of the difficulties associated with resolving the structures and obtaining consistent and accurate cell-dimensions for uranyl oxide hydrate minerals such as masuyite and vandendriesscheite (Deliens 1977b, Christ & Clark 1960, Frondel 1958).

Ianthinite

Schoepite can form by oxidation of ianthinite (Deliens 1977a, Guillemin & Protas 1959). The structure of ianthinite is unknown but may be similar to that of billietite (Finch & Ewing 1994). The conversion of ianthinite to schoepite occurs with little or no apparent strain. Oxidation proceeds as thin filaments of schoepite appear within ianthinite and grow preferentially along *b* (Schoep & Stradiot 1947). As the degree of oxidation of ianthinite increases, the filaments of schoepite coalesce until the entire crystal of ianthinite has been replaced by schoepite. This is accompanied by a change from dark purple ianthinite to yellow schoepite and by a continuous increase in $2V_\alpha$ from approximately 60° in ianthinite to approximately 75° in schoepite (Schoep & Stradiot 1947). The U^{4+} ions in ianthinite may occupy $U\phi_7$ polyhedra in the structural sheet, as reported recently for synthetic $U(UO_2)(PO_4)_2$ (Bénard *et al.* 1994). This is compatible with a protasite-type sheet and a U^{4+}:U^{6+} ratio of 1:5.

Acknowledgements

The authors are grateful to G. Mast of the Geology Museum at the Colorado School of Mines and to Dr. M. Deliens of the Institut Royal des Sciences Naturelles de Belgique and the Musée Royal de l'Afrique Centrale, Tervuren, for the loan of the schoepite samples. This work is supported by the Natural Sciences and Engineering Research Council of Canada. Early parts of this work were supported by the Swedish Nuclear Fuel and Waste Management Co. (SKB). RJF gratefully acknowledges an NSERC International Fellowship, and FCH was supported by NSERC Operating, Major Equipment and Infrastructure grants. Financial support for RCE was provided by DOE–BES (grant no. DE–FG03–95ER1450). The manuscript benefitted from careful reviews by S. Menchetti and C. Gramaccioli.

References

ÅBERG, M. (1978): The crystal structure of hexaaqua-tri-μhydroxo-μ_3-oxo-triuranyl(VI) nitrate tetrahydrate, $[(UO_2)_3O(OH)_3(H_2O)_6]NO_3{\cdot}4H_2O$. *Acta Chem. Scand.* **A32**, 101-107.

ARNBERG, L., HOVMÖLLER, S. & WESTMAN, S. (1976): On the significance of "non-significant" reflections. *Acta Crystallogr.* **A35**, 497-499.

BARAN, V. (1992): *Uranium–Oxygen Chemistry.* Nuclear Research Institute, Řež, Czech Republic.

BÉNARD, P., LOUÖR, D., DACHEUX, N., BRANDEL, V. & GENET, M. (1994): $U(UO_2)(PO_4)_2$, a new mixed-valence uranium orthophosphate: *ab initio* structure determination from powder diffraction data and optical and x-ray photoelectron spectra. *Chem. Materials* **6**, 1049-1058.

BIGNAND, C. (1955): Sur les propriétés et les synthèses de quelques minéraux uranifères. *Bull. Minéral.* **78**, 1-26.

BILLIET, V. & DE JONG, W.F. (1935): Schoepiet en Becquereliet. *Natuurwetenschappelijk Tijdschrift Ned-Indië* **17**, 157-162.

BROWN, I.D. & ALTERMATT, D. (1985): Bond-valence parameters obtained from a systematic analysis of the Inorganic Structure Data Base. *Acta Crystallogr.* **B41**, 244-247.

________ & WU, KANG KUN (1976): Empirical parameters for calculating cation–oxygen bond valences. *Acta Crystallogr.* **B32**, 1957-1959.

BRUNO, J., CASAS, I., CERA, E., EWING, R.C., FINCH, R.J. & WERME, L.O. (1995): The assessment of the long-term evolution of the spent nuclear fuel matrix by kinetic, thermodynamic and spectroscopic studies of uranium minerals. *In* Scientific Basis for Nuclear Waste Management XVIII (T. Murakami & R.C. Ewing, eds.). *Materials Research Soc. Proc.* **353**, 633-639.

BURNS, P.C., MILLER, M.L. & EWING, R.C. (1996): Uranyl minerals and inorganic phases: a comparison and hierarchy of crystal structures. *Can. Mineral.* **34**, 845-880.

ČEJKA, J. & URBANEC, Z. (1990): *Secondary Uranium Minerals.* Academia, Czechoslovak Academy of Sciences, Prague, Czech Republic.

CHRIST, C.L. (1965): Phase transformations and crystal chemistry of schoepite. *Am. Mineral.* **50**, 235-239.

________ & CLARK, J.R. (1960): Crystal chemical studies of some uranyl oxide hydrates. *Am. Mineral.* **45**, 1026-1061.

DEBETS, P.G. & LOOPSTRA, B.O. (1963): On the uranates of ammonium. II. X-ray investigation of the compounds in the system NH_3–UO_3–H_2O. *J. Inorg. Nucl. Chem.* **25**, 945-953.

DELIENS, M. (1977a): Associations de minéraux secondaires d'uranium à Shinkolobwe (région du Shaba, Zaïre). *Bull. Minéral.* **100**, 32-38.

________ (1977b): Review of the hydrated oxides of U and Pb, with new X-ray powder data. *Mineral. Mag.* **41**, 51-57.

EVANS, H.T., JR. (1963): Uranyl ion coordination. *Science* **141**, 154-158.

EWING, R.C. (1993): The long-term performance of nuclear waste forms: natural materials – three case studies. *In* Scientific Basis for Nuclear Waste Management XVI (C.G. Interante & R.T. Pabalan, eds.). *Materials Research Soc. Proc.* **294**, 559-568.

FINCH, R.J. & EWING, R.C. (1992): The corrosion of uraninite under oxidizing conditions. *J. Nucl. Materials* **190**, 133-156.

________ & ________ (1994): Formation, oxidation and alteration of ianthinite. *In* Scientific Basis for Nuclear Waste Management XVI (A. Barkatt & R.A. von Konynenburg, eds.). *Materials Research Soc. Proc.* **333**, 625-630.

________, MILLER, M.L. & EWING, R.C. (1992): Weathering of natural uranyl oxide hydrates: schoepite polytypes and dehydration effects. *Radiochim. Acta* **58/59**, 433-443.

FORSYTH, R.S. & WERME, L.O. (1992): Spent fuel corrosion and dissolution. *J. Nucl. Materials* **190**, 3-19.

FRONDEL, C. (1958): Systematic mineralogy of uranium and thorium. *U.S. Geol. Surv., Bull.* **1064**.

GUILLEMIN, C. & PROTAS, J. (1959): Ianthinite et wyartite. *Bull. Minéral.* **82**, 80-86.

HAWTHORNE, F.C. (1992): The role of OH and H_2O in oxide and oxysalt minerals. *Z. Kristallogr.* **201**, 183-206.

________ (1994): Structural aspects of oxides and oxysalt crystals. *Acta Crystallogr.* **B50**, 481-510.

HIRSHFELD, F.L. & RABINOVICH, D. (1973): Treating weak reflexions in least-squares calculations. *Acta Crystallogr.* **A29**, 510-513.

HOEKSTRA, H.R. & SIEGEL, S. (1973): The uranium trioxide – water system. *J. Inorg. Nucl. Chem.* **35**, 761-779.

JOHNSON, L.H. & WERME, L.O. (1994): Materials characteristic and dissolution behavior of spent nuclear fuel. *Materials Res. Soc. Bull.* **XIX**(12), 24-27.

LOOPSTRA, B.O. & RIETVELD, H.M. (1969): The structures of some alkaline-earth metal uranates. *Acta Crystallogr.* **B25**, 787-791.

MEREITER, K. (1979): The crystal structure of curite, $[Pb_{6.56}(H_2O,OH)_4][(UO_2)_8O_8(OH)_6]_2$. *Tschermaks Mineral. Petrol. Mitt.* **26**, 279-292.

MILLER, M.L., FINCH, R.J., BURNS, P.C. & EWING, R.C. (1996): Description and classification of uranium oxide hydrate sheet topologies. *J. Materials Research* (in press).

PAGOAGA, M.K. (1983): *The Crystal Chemistry of the Uranyl Oxide Hydrate Minerals.* Ph.D. thesis, Univ. of Maryland, College Park, Maryland.

________, APPLEMAN, D.E. & STEWART, J.M. (1987): Crystal structures and crystal chemistry of the uranyl oxide hydrates becquerelite, billietite, and protasite. *Am. Mineral.* **72**, 1230-1238.

PETERS, J.-M. (1967): Synthèses et étude radiocristallographique d'uranates synthétiques du type oxyde double d'uranyl. *Mém. Soc. Roy. Sci. Liège, sér.* **5**, **14**(3), 5-57.

PIRET, P. (1985): Structure cristalline de la fourmariérite, $Pb(UO_2)_4O_3(OH)_4{\cdot}4H_2O$. *Bull. Minéral.* **108**, 659-665.

________, DELIENS, M., PIRET-MEUNIER, J. & GERMAIN, G. (1983): La sayrite, $Pb_2[(UO_2)_5O_6(OH)_2]{\cdot}4H_2O$, nouveau minéral; propriétés et structure cristalline. *Bull. Minéral.* **106**, 299-304.

PIRET-MEUNIER, J. & PIRET, P. (1982): Nouvelle détermination de la structure cristalline de la becquerelite. *Bull. Minéral.* **105**, 606-610.

PROTAS, J. (1959): Contribution à l'étude des oxydes d'uranium hydratés. *Bull. Minéral.* **82**, 239-272.

SCHOEP, A. (1932): The specific gravity and chemical composition of becquerelite and schoepite. *Mus. Congo Belge. Ann. (Minéralogie)* **I**, *Fasc.* **III**, 5-7.

________ & STRADIOT, S. (1947): Paraschoepite and epiianthinite, two new uranium minerals from Shinkolobwe (Belgian Congo). *Am. Mineral.* **32**, 344-350.

SMITH, D.K., JR. (1984): Uranium mineralogy. *In* Uranium Geochemistry, Mineralogy, Geology, Exploration and Resources (B. DeVivo, F. Ippolito, G. Capaldi & P.R. Simpson, eds.). Institute of Mining and Metallurgy, London, U.K. (43-88).

SOBRY, R. (1973): Étude des uranates hydratés. I. Propriétés radiocristallographiques des uranates hydratés de cations bivalents. *J. Inorg. Nucl. Chem.* **35**, 1515-1524.

STROES-GASCOYNE, S., JOHNSON, L.J., BEELEY, P.A. & SELLINGER, D.M. (1985): Dissolution of used CANDU fuel at various temperatures and redox conditions. *In* Scientific Basis for Nuclear Waste Management IX (L.O Werme, ed.). *Materials Research Soc. Proc.* **50**, 317-326.

TAYLOR, J.C. (1971): The structure of the α form of uranyl hydroxide. *Acta Crystallogr.* **B27**, 1088-1091.

WADSTEN, T. (1977): The oxidation of polycrystalline uranium dioxide in air at room temperature. *J. Nucl. Materials* **64**, 315.

WALKER, T.L. (1923): Schoepite, a new uranium mineral from Kasolo, Belgian Congo. *Am. Mineral.* **8**, 67-69.

WANG, R. & KATAYAMA, J.B. (1982): Dissolution mechanism for UO_2 and spent fuel. *Nucl. Chem. Waste Management* **3**, 83-90.

WILSON, A.J.C. (1976): Statistical bias in least-squares refinement. *Acta Crystallogr.* **A32**, 994-996.

WRONKIEWICZ, D.J., BATES, J.K., GERDING, T.J., VELECKIS, E. & TANI, B.S. (1992): Uranium release and secondary phase formation during unsaturated testing of UO_2 at 90°C. *J. Nucl. Materials* **190**, 107-127.

Received January 3, 1996, revised manuscript accepted June 3, 1996.